Electronic Supplementary Information for

Ring-locking Enables Selective Anhydrosugar Synthesis from Carbohydrate Pyrolysis

Li Chen[a], Jin-mo Zhao[b], Sivaram Pradhan[a], Bruce E. Brinson[b], Gustavo E. Scuseria[b], Z. Conrad Zhang[c*], Michael S. Wong[a,b,d,e*]

[a]Department of Chemical and Biomolecular Engineering, Rice University, Houston, TX 77005, USA.
[b]Department of Chemistry, Rice University, Houston, TX 77005, USA.
[c]Dalian National Laboratory of Clean Energy, Dalian Institute of Chemical Physics, Dalian, Liaoning 116023, China.
[d]Department of Civil and Environmental Engineering, Rice University, Houston, TX 77005, USA.
[e]Department of Materials Science and NanoEngineering, Rice University, Houston, TX 77005, USA.

*Correspondence to: mswong@rice.edu, zczhang@dicp.ac.cn

Thin-film characterization

The thin films were imaged using an FEI Quanta 400 environmental scanning secondary electron microscope (ESEM) (Hillsboro, OR), equipped with an EDAX™ (Trenton, NJ) energy dispersive X-ray spectrometer (EDS) fitted with a Super UTW™ 0.3-nm window and SiLi detector, which was operated at 20 KV with a chamber pressure of 3 Torr (H_2O). Quartz tubes, containing the thin films of dried sample films on the inner wall, were carefully scribed and fractured to expose the pristine film-substrate interface, then mounted with their cylindrical axis parallel to the electron beam. EDS confirmed the presence of a carbon-based film before and after images were acquired.

Pyrolysis thin-film experiments analysis

This paper uses the Pyrolysis number (*Py*) and Biot number (*Bi*) to compare conduction time scale ($\tau_{conduction}$) and convection time scale ($\tau_{convection}$) with reaction time scale ($\tau_{reaction}$) (eqn (1)-(3)). The criteria for kinetically limited isothermal reaction regime is $\tau_{reaction} >> (\tau_{convection}, \tau_{conduction})$, which requires $Bi << 1$ and $Py >> 1$.

$$Py^{I} = \frac{\tau_{reaction}}{\tau_{conduction}} = \frac{\lambda}{\rho C_P L^2 k} \tag{1}$$

$$Py^{II} = \frac{\tau_{reaction}}{\tau_{convection}} = \frac{h_s}{\rho C_P L k} \tag{2}$$

$$Bi = \frac{\tau_{conduction}}{\tau_{convection}} = \frac{h_s L}{\lambda} \tag{3}$$

The physical property values and kinetics data used are as follows: thermal conductivity of cellulose: $\lambda = 0.2426\ W/(m \cdot K)$[1]; density of cellulose: $\rho = 420\ kg/m^3$ $\rho = 420\ kg/m^3$[1]; heat capacity of cellulose: $C_P = 2300\ J/(kg \cdot K)$[1]; enthalpy variation for cellulose pyrolysis: $\Delta H_{rxn} = 794\ kJ/mol$[1]; overall reaction rate constant for cellulose pyrolysis: $k = 310\ s^{-1}$, calculated from [2]; heat transfer coefficient between thin film and hot surface: $h_s = 2000\ W/(m^2 \cdot K)$[3]; and characteristic length: L. SEM imaging showed all of the film thicknesses (L) were less than 10^{-5} m, though usually closer to ~10^{-6} m. They were thin enough to satisfy the conditions of Bi < 0.1 ($\tau_{conduction} << \tau_{convection}$) and $Py^{I} > 10$ ($\tau_{reaction} >> \tau_{conduction}$). For example, thicknesses L = 10^{-5} m and 10^{-6} m corresponded to Bi = 8.24×10^{-2} and 8.24×10^{-3}, respectively (and $Py^{I} = 8.10$ and 8.10×10^{2}). The corresponding Py^{II} were 0.67 and 6.68, coming close to the condition of $Py^{II} > 10$ (or

$\tau_{reaction} >> \tau_{convection}$). The relatively large standard deviation values for some of the selectivity/conversion data points (in Figure 2, for example) could be due to sensitivity to film thickness variations. Importantly, our pyrolysis experiments were outside the convection-limited, conduction-limited, and non-isothermal&kinetically-controlled regimes (shown in M. Mettler *et al.*'s Py-Bi diagram[3]).

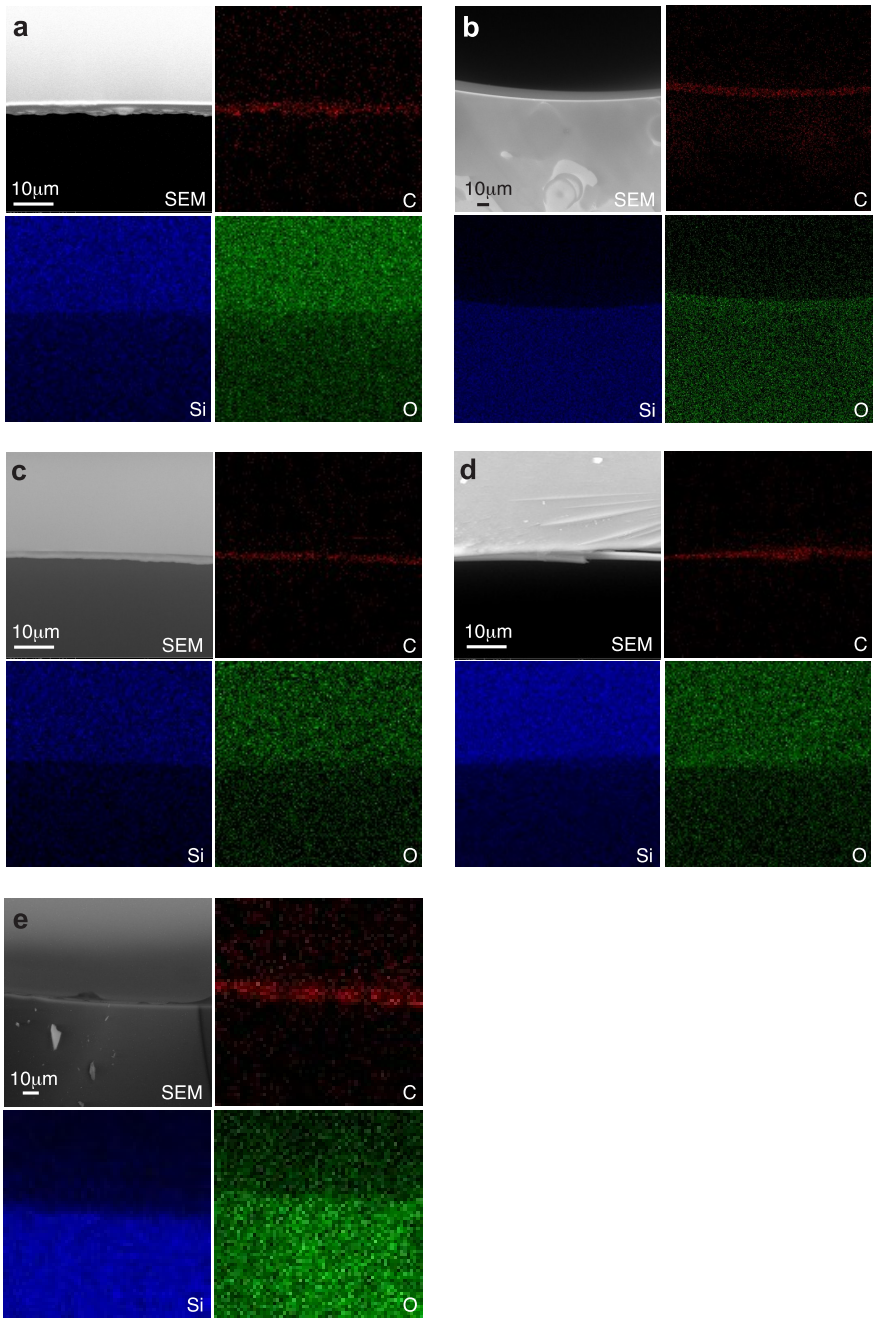

Figure S1. The scanning electron microscopy (SEM) images of (**a**) β-MG, (**b**) α-MG, (**c**) β-PG, (**d**) α-PG, and (**e**) β-G. Due to high susceptibility to electron beam damage, the

elemental maps for β-G were recorded at lower magnification, lower resolution and withshorter dwell times to minimize beam damage during the collection period.

Pyroprobe coupled with GC/FID system

For each pyrolysis experiment, helium was used as the inert gas for the pyrolyzer and carrier gas for the Pyrolysis-GC/FID system. The sample tube (Fig. S2c) with two open ends was placed inside the sample holder ("pyroprobe") comprising a coiled platinum heating filament. During pyrolysis, the gaseous products exited the sample tube ends and transported by the carrier gas into a heated chamber and then into the GC/FID.

Fig. S2a shows the temperature profiles for a pyrolysis run. In stage 1, the pyroprobe (sample holder) temperature was equilibrated at 50 °C (T_{low_rest}) before it ramped (~7 °C/s) to 250 °C (T_{high_rest}). The temperature was held for 10 s at 250 °C, before the temperature ramped (20,000 °C/sec) to the pyrolysis temperature (600 °C) (stage 2). The pyroprobe was held at the pyrolysis temperature for 20 s (Δt_1), after which it cooled to T_{high_rest}. For the remainder of stage 2 (Δt_2=60 s), the pyroprobe was kept at 250 °C with He gas flowing continuously into the GC-FID. During stage 3, the pyroprobe was cooled to T_{low_rest}.

In the GC/FID, constant carrier gas flow rate of 1.0 mL min^{-1} was maintained through the capillary column (VF-1701ms, 60m×0.250mm×0.250μm). The septum purge flow was 2.5mL/min. The total flow for the GC is the sum of septum purge flow (2.5 mL/min), column flow (1 mL/min), and split vent flow (= split ratio × column flow). The gas flow rate for the pyrolyzer was controlled by the GC, so the total flow to the GC equals the flow of through the pyrolyzer. The total flow (and therefore the flow through the pyrolyzer) was controlled by changing the split ratio. The GC oven temperature was first equilibrated at 37 °C for 3 min, before it ramped to 130 °C at a rate of 10 °C/min, and ramped to 250 °C at 3 °C/min and held at this temperature for 15 min. The total analysis time was 62.3 min. Sugar conversion was controlled by adjusting the carrier gas flow and sample heating time. Heating times between 0.1 and 20 sec (at a 100:1 split ratio) achieved the sugar conversions of <20%. GC split ratios between 100:1 and 10:1 (at a heating time of 20 sec) achieved higher conversions of >20%. The schematic of the Pyrolyzer, splitter, GC and the carrier gases is shown in Fig. S2 and the various operational conditions are listed in Table S3.

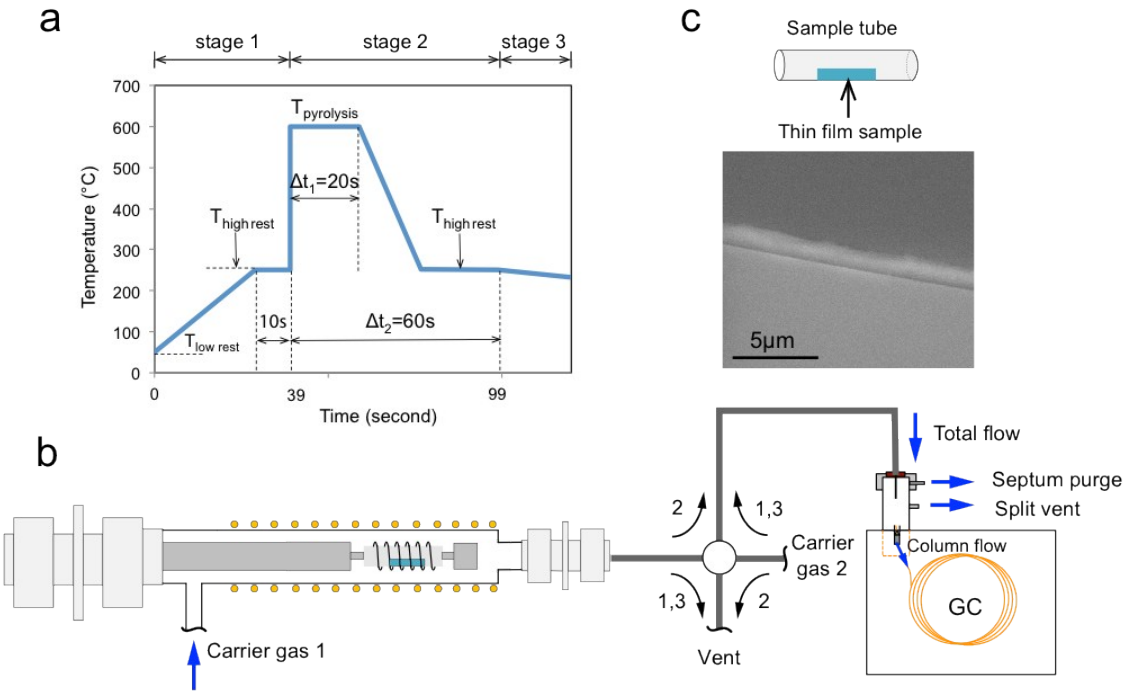

Figure S2. Diagram for thin-film pyrolysis. **a**, Temperature profile of the pyroprobe for a pyrolysis run, which contains three stages. **b**, Schematics for the pyrolyzer and GC. In stages 1 and 3, carrier gas 1 flows to vent, and the carrier gas 2 flows into GC; while in stage 2, the carrier gas 1 flows into the GC directly and the carrier gas 2 flows to the vent. **c**, quartz tube with thin film sample inside (on the top), SEM image showing an edge view of a β-PG film on SiO_2.

Methyl-D-glucoside synthesis using complex carbohydrates

The synthesis was carried out with more complex substrates, such as cellulose [3], Whatman filter paper (grade 42) and sterile absorbent cotton (USP grade, U.S. cotton). These substrates were washed to remove the mineral contaminants [4] prior to the synthesis: 1 g of the substrate was stirred in 20 mL of HNO_3 (0.1N) for 5 min, filtered, and the solid residue was rinsed with 60 mL DI water. The glycosylation procedure was similarly carried using these washed substrates to synthesize the methyl glucoside crude. The methyl glucoside yield was very low due to the lower reactivity of these substrates, and so the reactions were next performed at a higher temperature (~210 °C) using a Parr reactor [5]. 100 mg of pre-washed and ground substrate, and 10 mg Amberlyst-15 catalyst were suspended into 4 mL of methanol. The solution mixture was charged into the 16 mL Teflon-lined stainless steel reactor. The reactor was placed in a preheated oven at 210 °C for 30 min. After the reaction, the reactor was cooled immediately by ice bath to quench further reaction. The Amberlyst-15 and unreacted biomass were recovered using a syringe filter, dried at 110 °C for 1 h, and weighed to estimate the conversion of the substrate. The filtrate was concentrated to 6 mL and analyzed by HPLC. 20 μl of the filtrate was transferred into a quartz tube and dried under vacuum to form the thin film for pyrolysis.

Conversion for biomass ($X_{cellulose}, X_{filter-paper}, X_{cotton}$) was calculated by the weight difference before and after reaction.

Methyl-glucoside yield ($Y_{\alpha-MG}, Y_{\beta-MG}$) calculation:

$$Y_{\alpha-MG} = \frac{moles\ of\ HPLC\ detected\ \alpha-MG}{initial\ moles\ of\ C_6H_{10}O_5\ unit\ in\ substrate} \times 100\% \tag{16}$$

$Y_{\beta-MG}$ was calculated similarly.

β-MG (Structure I)

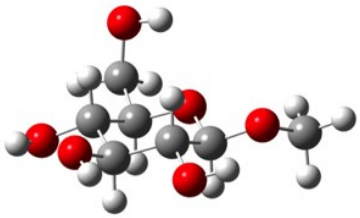

β-MG (Structure III)

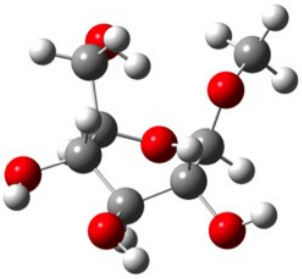

β-MG (Structure V)

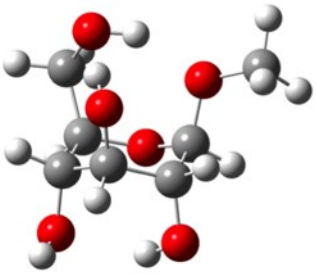

β-MG (Structure VI)

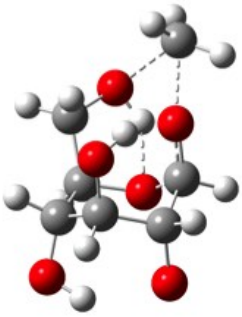

β-MG (Structure VII)

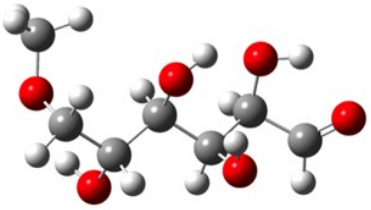

β-MG (Structure vi)

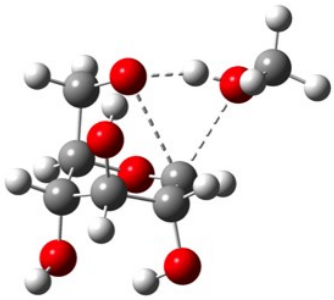

β-MG (Structure vii)

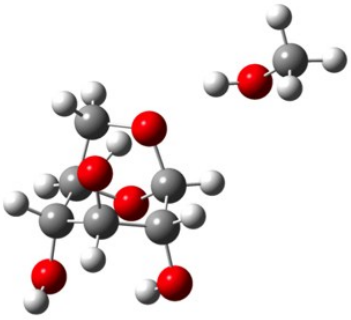

β-PG (Structure I)

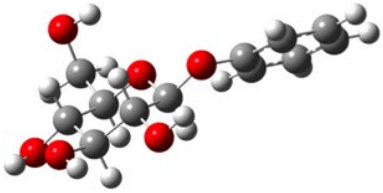

β-PG (Structure III)

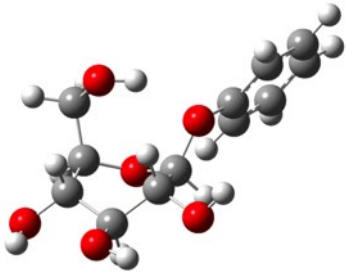

(continued in next page)

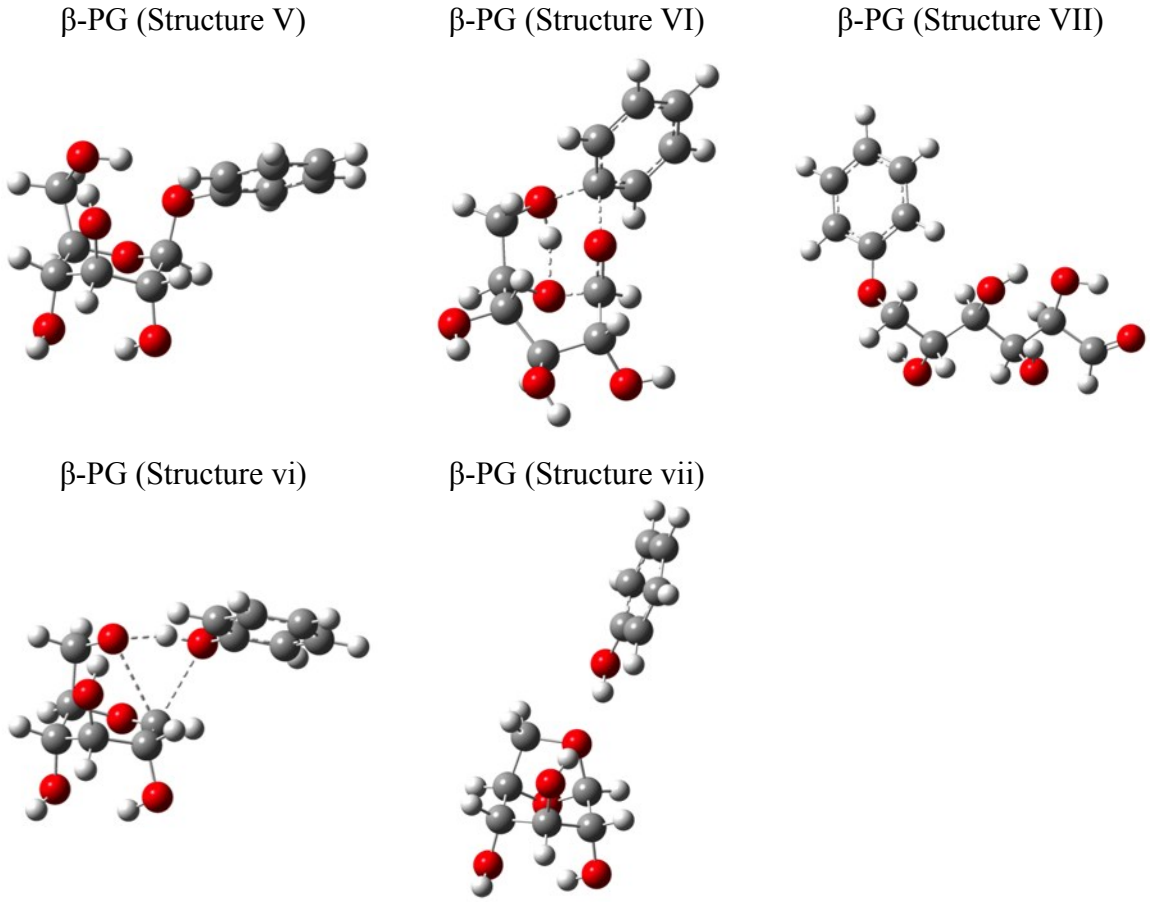

Figure S3. Representative 3-D structures used in β-MG and β-PG ring opening and LGA formation pathway calculation, optimized at the B3LYP/6-31G(d,p) level of theory.

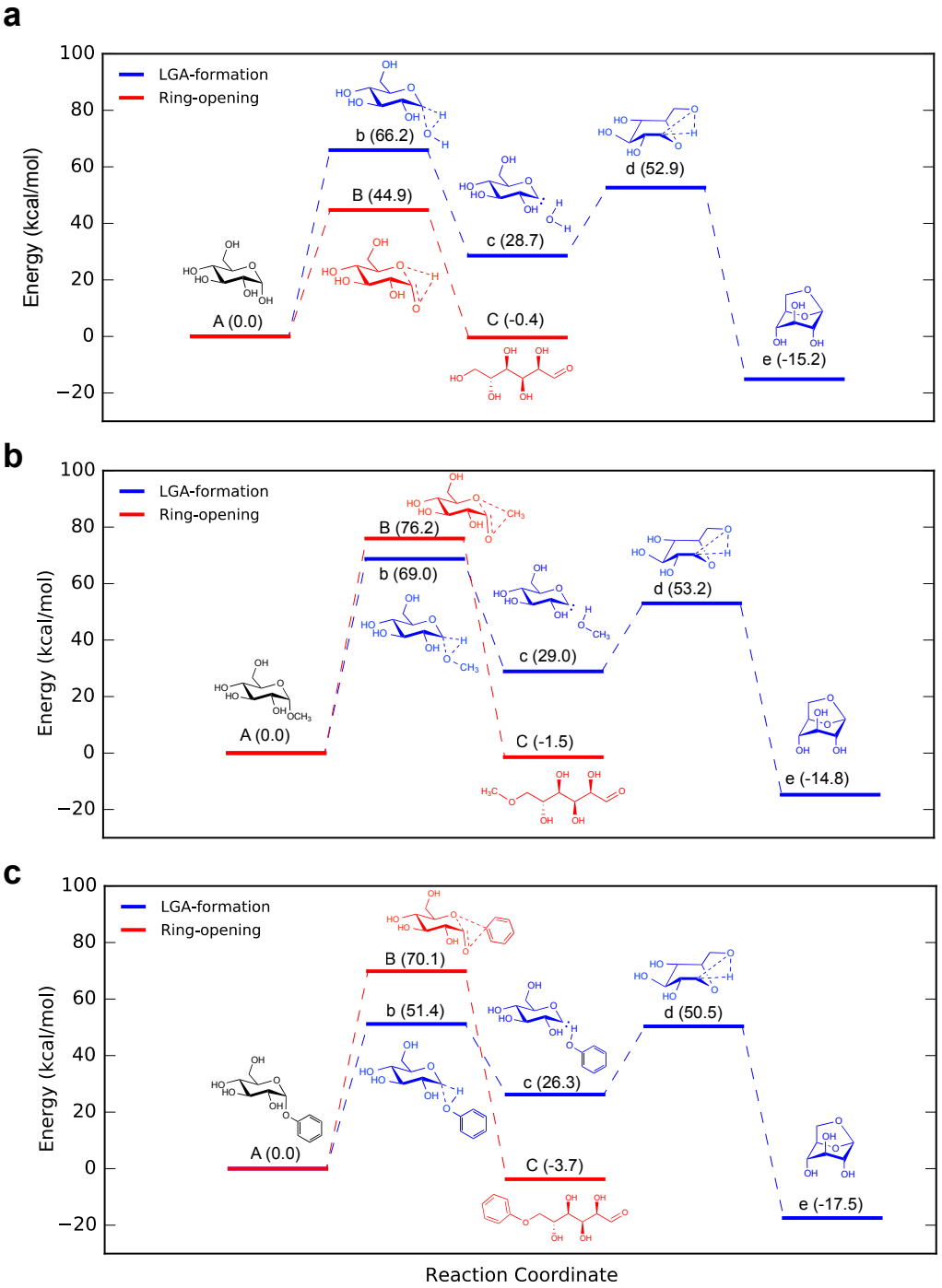

Figure S4. Relative Gibbs free energy profile for LGA formation reaction and ring-opening reaction paths for (**a**) α-G, (**b**) α-MG and (**c**) α-PG pyrolysis at 600 °C. Structures B, b and d are the rate-determining transition states. 3-D structures are shown in Fig. S5.

α-G (Structure A)

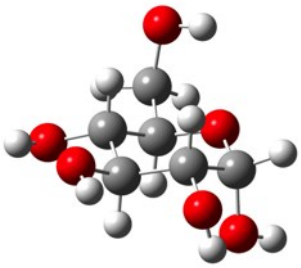

α-G (Structure B)

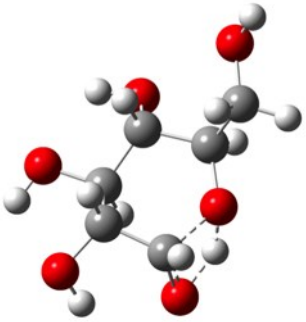

α-G (Structure C)

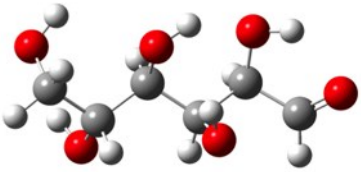

α-G (Structure b)

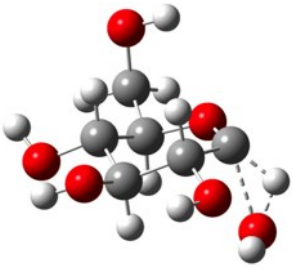

α-G (Structure c)

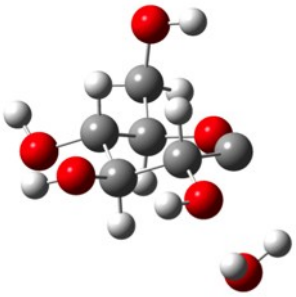

α-G (Structure d)

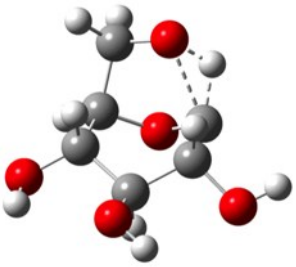

α-G (Structure e)

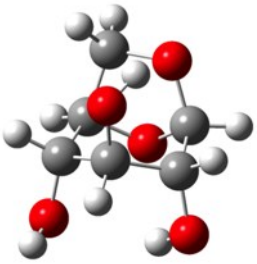

α-MG (Structure A)

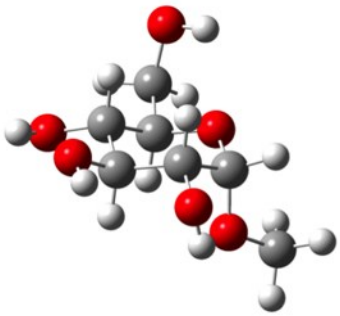

α-MG (Structure B)

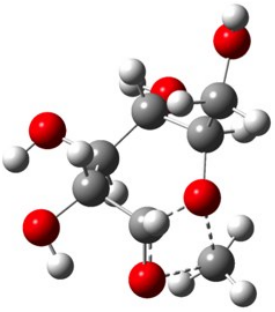

(Continued in next page)

130

α-MG (Structure C)

α-MG (Structure b)

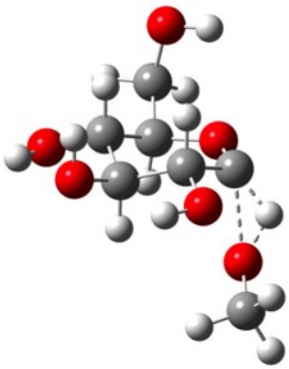

α-MG (Structure c)

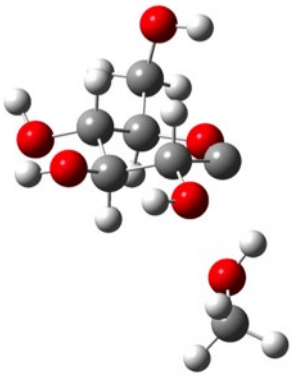

α-MG (Structure d)

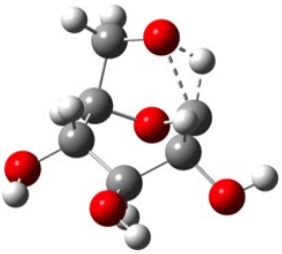

α-MG (Structure e)

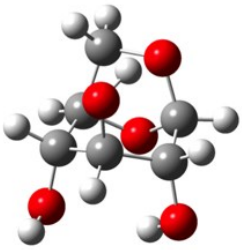

α-PG (Structure A)

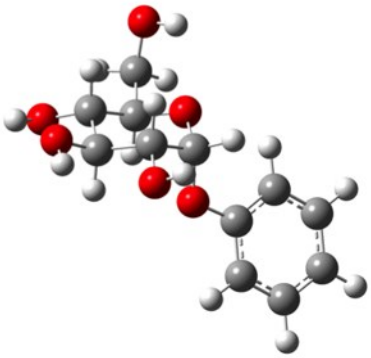

α-PG (Structure B)

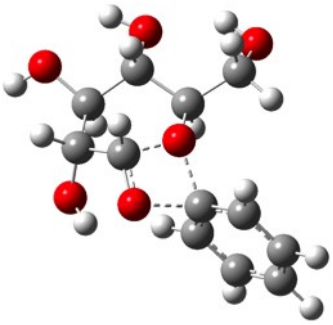

α-PG (Structure C)

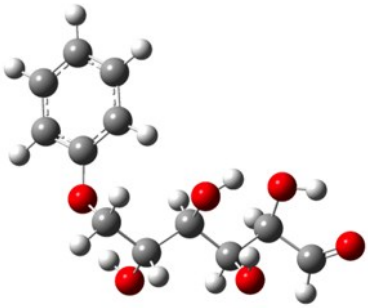

α-PG (Structure b)

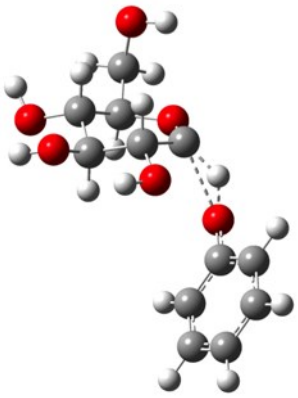

(Continued in next page)

131

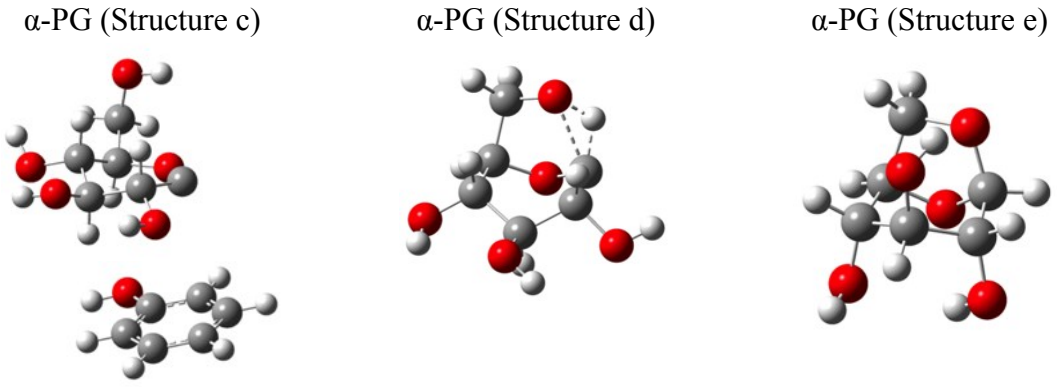

Figure S5. Representative 3-D structures used in α-G, α-MG and α-PG ring opening and LGA formation pathway calculation, optimized at the B3LYP/6-31G(d,p) level of theory.

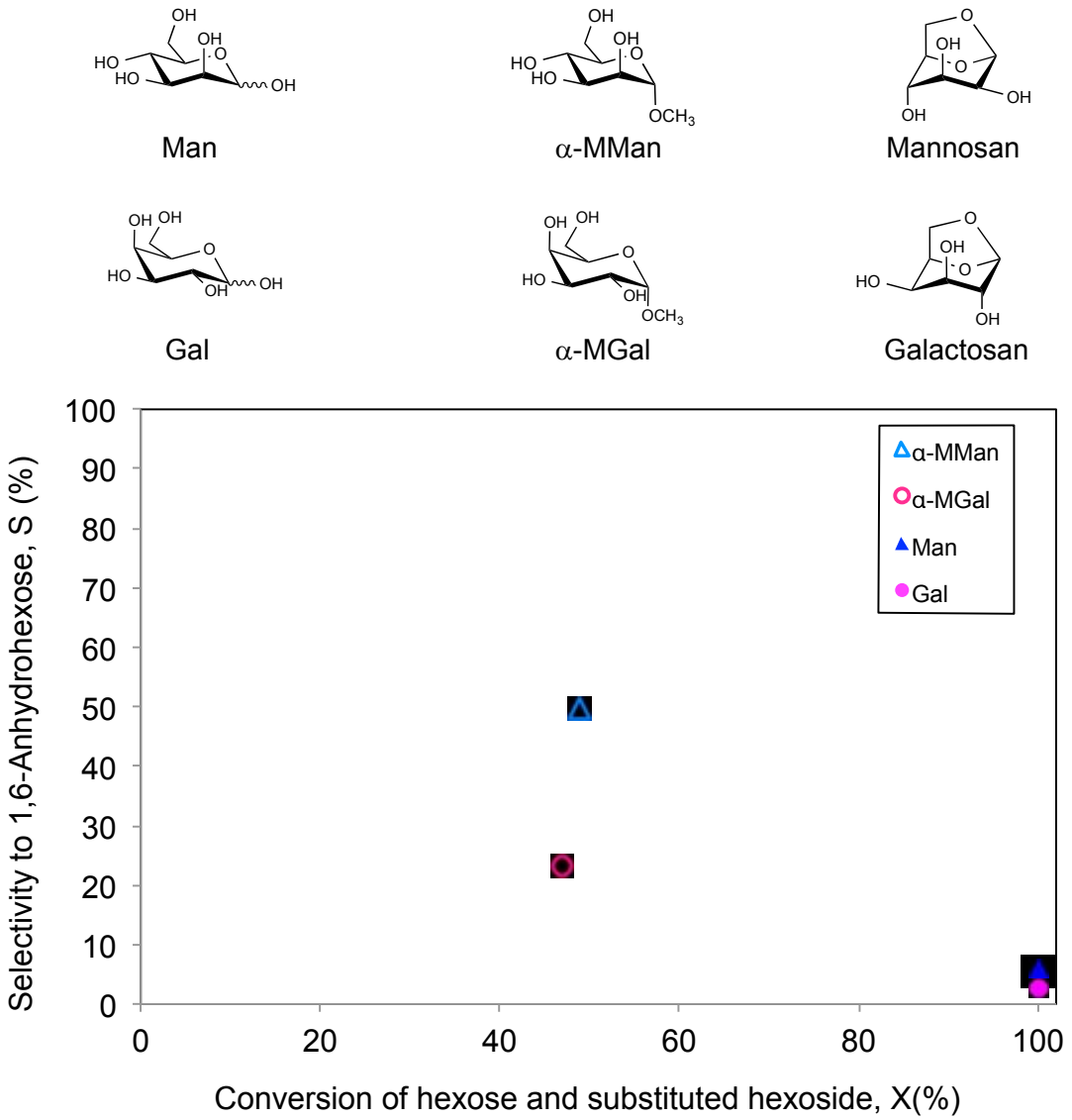

Figure S6. Selectivity to 1,6-anhydrohexoses from pyrolysis of methyl-α-D-mannoside (α-MMan), methyl-α-D-galactoside (α-MGal), D-mannose (Man), and D-galactose (Gal) at 600 °C. Flash pyrolysis reaction condition: 600 °C, thin film sample size = 32 μg, heating time = 20 s, carrier gas split ratio = 100:1, Agilent 7890B gas chromatograph with 5977A mass spectrometer detector.

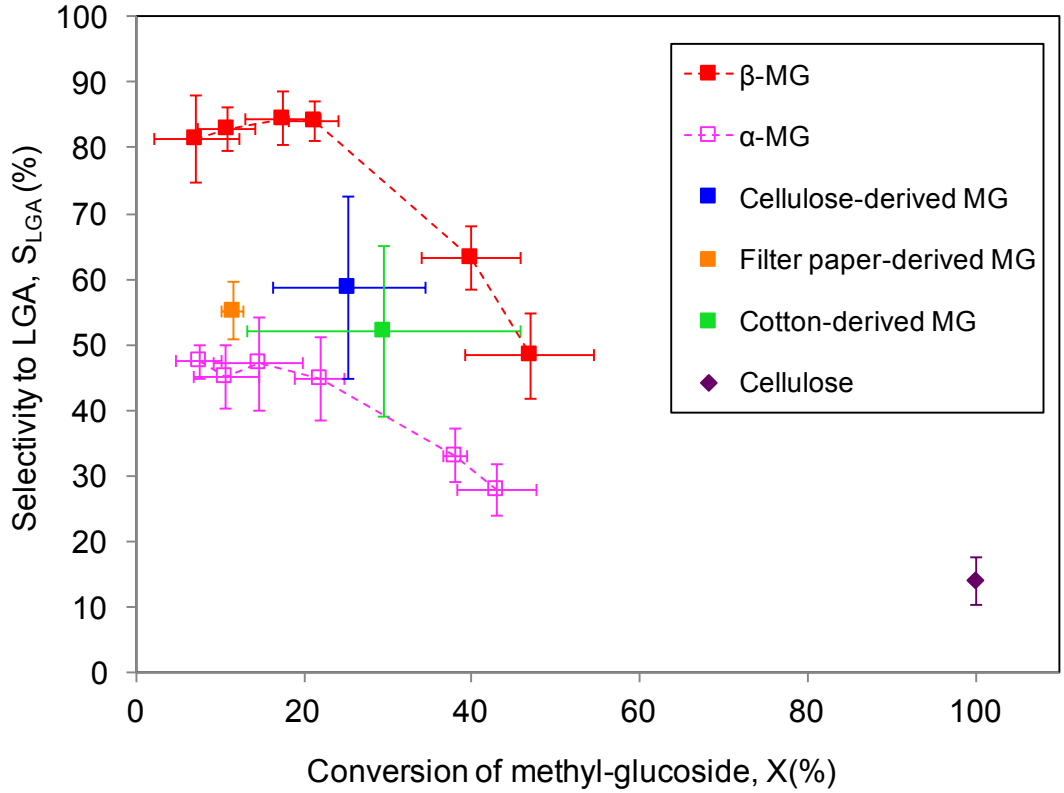

Figure S7. LGA selectivity from pyrolysis of crude methyl-D-glucoside prepared from various complex carbohydrates. Data for β-MG and α-MG are from Fig. 2. Pyrolysis temperature = 600 °C, heating time of 20 s, carrier gas split ratio = 100:1.

Table S1. LGA yields reported at different temperatures from cellulose thin-film pyrolysis, and LGA selectivities calculated from reference [6] data. Reference [7] reports similar trends in pyrolysis of cellulose powders.

Temperature (°C)	LGA carbon yield (%)	LGA carbon selectivity (%)
400	29±1	32.6
500	27±2	28
550	22±0.7	24

Table S2. Summary of pyrolysis products in thin-film pyrolysis experiments at 600 °C, split ratio = 100:1, probe heating time = 20 sec.

No.	Compound	Reference	Molar mass (g mol^{-1})	Structure	Found from β-G pyrolysis	Found from β-MG pyrolysis	Found from α-MG pyrolysis	Found from β-PG pyrolysis	Found from α-PG pyrolysis
1	Methanol	-	32	H_3C—OH		Yes	Yes		
2	Acetone; Propanone	[4]	58		Yes				
3	Glycolaldehyde; 2-hydroxyacetaldehyde	[3,4]	60	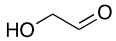	Yes				
4	Furfural; Furan-2-carbaldehyde	[3,4]	96	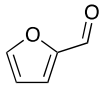	Yes				
5	Glyceraldehyde; 2,3-dihydroxypropanal	[8]	90	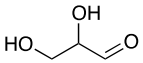	Yes				

6	Phenol	-	94	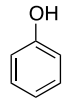				Yes	Yes
7	HMF; Hydroxymethylfurfural; 5-hydroxymethyl-2-furaldehyde	[3,4]	126	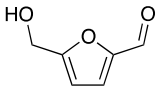	Yes				
8	ADGH; 1,5-anhydro- 4-deoxy-D- glycero-hex- 1-en-3-ulose	[3,9]	144	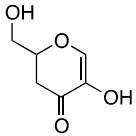			Yes		Yes
9	Unidentified anhydrosugar	-	N.A	N.A.	Yes				
10	LGA; Levoglucosan; 1,6-anhydro-β-D-glucopyranose; 6,8-dioxabicyclo [3.2.1] octane-2,3,4-triol	[3,4]	162	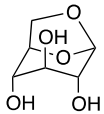	Yes	Yes	Yes	Yes	Yes
11	1,6-anhydro-β-D-glucofuranose; 2,8-dioxabicyclo [3.2.1] octane-4, 6,7-triol	[3,4]	162	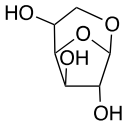	Yes				

Table S3. Relative Gibbs free energies of important intermediates and transition states. All of the quantum mechanical and statistical mechanical computations were performed using the Gaussian 09 program package with DFT method. Basis set: B3LYP/6-31G(d,p) at 600 °C.

	ΔG (kcal/mol)				
Reaction	I	III	V	vi	vii
β-G→LGA	0.0	5.0	7.0	47.0	-15.7
β-MG→LGA	0.0	5.3	5.9	46.6	-15.4
β-PG→LGA	0.0	3.6	8.3	40.3	-15.9
	I	III	V	VI	VII
β-G ring opening	0.0	5.0	7.0	37.3	-4.2
β-MG ring opening	0.0	5.3	5.9	86.2	-2.1
β-PG ring opening	0.0	3.6	8.3	85.0	-2.2
	A	b	c	d	e
α-G→LGA	0.0	66.2	28.7	52.9	-15.2
α-MG→LGA	0.0	69.0	29.0	53.2	-14.8
α-PG→LGA	0.0	51.4	26.3	50.5	-17.5
	A	B	C		
α-G ring opening	0.0	44.9	-0.4		
α-MG ring opening	0.0	76.2	-1.5		
α-PG ring opening	0.0	70.1	-3.7		

Table S4. Composition of the crude methyl-D-glucoside prepared from various complex carbohydrates, and corresponding LGA selectivities from its pyrolysis. Pyrolysis temperature = 600 °C, heating time of 20 s, carrier gas split ratio = 100:1. For comparison, LGA yield from pyrolysis of untreated cellulose was 14% at 100% conversion.

Synthesis of crude MG							Pyrolysis of crude MG		
Substrate	Substrate conversion (wt%)	α-MG yield (wt%)	β-MG yield (wt%)	Crude MG composition			LGA selectivity (%)	LGA yield (%)	MG pyrolysis conversion (%)
				α-MG (wt%)	β-MG (wt%)	Other (wt%)			
Cellulose	24±4	6±0.6	4±0.4	23±4	15±3	62	59±14	15±8	25±9
Filter paper	22±7	4±0.2	3±0.1	24±6	16±4	61	55±4	6±1	12±1
Cotton	20±4	4±0.5	2±0.4	20±2	13±1	68	52±13	16±10	30±16

References

1 C. Di Blasi, *Biomass and Bioenergy*, 1994, **7**, 87–98.

2 R. Vinu and L. J. Broadbelt, *Energy Environ. Sci.*, 2012, **5**, 9808.

3 M. S. Mettler, S. H. Mushrif, A. D. Paulsen, A. D. Javadekar, D. G. Vlachos and P. J. Dauenhauer, *Energy Environ. Sci.*, 2012, **5**, 5414.

4 P. R. Patwardhan, J. A. Satrio, R. C. Brown and B. H. Shanks, *J. Anal. Appl. Pyrolysis*, 2009, **86**, 323–330.

5 W. Deng, M. Liu, Q. Zhang, X. Tan and Y. Wang, *Chem. Commun. (Camb).*, 2010, **46**, 2668–70.

6 A. D. Paulsen, M. S. Mettler and P. J. Dauenhauer, *Energy & Fuels*, 2013, **27**, 2126–2134.

7 a. V. Bridgwater, D. Meier and D. Radlein, *Org. Geochem.*, 1999, **30**, 1479–1493.

8 T. R. Carlson, J. Jae, Y.-C. Lin, G. a. Tompsett and G. W. Huber, *J. Catal.*, 2010, **270**, 110–124.

9 F. Shafizadeh, R. H. Furneaux, T. T. Stevenson and T. G. Cochran, *Carbohydr. Res.*, 1978, **67**, 433–447.